

FIELD TESTS WITH LIBS SPECTROMETER ASSESSING LITHIUM, CESIUM, AND RUBIDIUM IN THE LACUSTRINE AND VOLCANOCLASTIC SEDIMENTS OF ERDŐBÉNYE, TOKAJ MOUNTAIN, HUNGARY

Mohammed Ali BELAY^{1,2}, János FÖLDESSY¹, László KUPI³, & Ferenc MÁDAI¹

¹*Institute of Geology and Mineralogy, University of Miskolc, Hungary*

²*Department of Mining Engineering, Addis Ababa Science and Technology University, Addis Ababa, Ethiopia, email: mohammed.ali@aastu.edu.et, phone: +251921530093*

³*Aurum Mineral Exploration consultancy, Budapest, Hungary*

Abstract: In this article, we aimed to analyse and evaluate the alkaline metals (such as Li, Cs, and Rb) enrichment in the lacustrine and volcanoclastic sediments of the Erdőbénye valley basin of north eastern Hungary using a field spectrometer and ICP-MS analysis methods in order to define a potential exploration target. The results are ambiguous and the consequences are summarized in this article. Alkaline metals such as Li, Cs, and Rb are essential for the 5G technology, production of batteries, various ceramics and glass products, as well as other crucial application areas in the current world. As a result, the demand for those elements is skyrocketing on a world-wide. A potential target area was selected to test the applicability of LIBS field spectrometer in this segment of industrial mineralization.

Key words: alkaline metal, lacustrine sediments, volcanoclastic sediment, basin, field spectrometry, ICP-MS

1. INTRODUCTION

The Erdőbénye valley basin is located in the northeast of Hungary. In this basin, there is a diatomite mine. Different scholars attempt to measure the concentration of Li, Cs and Rb in the area with different time and mechanism. The investigation was run to prospect the element Li in the basin using handheld field spectrometry (LIBS). However, good concentration of Cs and Rb were detected during the measurement.

Handheld Laser-Induced Breakdown Spectroscopy (LIBS) is a tool in which a quick, portable, in situ technique that used to detect the concentration of major and trace elements of a material on the spot. It can detect light elements such as Li, B, C, and Na, which XRF cannot (Senesi, 2017).

In hard rocks, lithium ore deposits include spodumene ($\text{LiAlSi}_2\text{O}_6$), lepidolite ($\text{K}(\text{Li},\text{Al})_3(\text{Si},\text{Al})_4\text{O}_{10}(\text{F},\text{OH})_2$), petalite ($\text{LiAlSi}_4\text{O}_{10}$), amblygonite ($(\text{Li},\text{Na})\text{Al}(\text{PO}_4)(\text{F},\text{OH})$), and eucryptite (LiAlSiO_4) and others. Li is found in sedimentary rocks as jadarite ($\text{LiNaSiB}_3\text{O}_7(\text{OH})$), illite, smectite, hectorite, and other minerals. Furthermore, it can be found in brines, such as in salars (Brine reservoirs),

oilfields, geothermal, and oceans, (Hart et al., 1973). Sediments that form sedimentary deposits typically have low consistency, and sometimes they are going to easily disintegrate when they are placed in water. The lithium doesn't make any bond in a crystal lattice at all, it would wash out by water in ionic form and go to form a brine deposit, (Grant, 2019).

Lithium in the sedimentary environment may be found as lithium chloride (LiCl), lithium hydroxide (LiOH), and lithium carbonate (Li_2CO_3) compounds as well as jadarite (Talens Peiró et al., 2013).

There are two distinct minerals of caesium, which are pollucite, a hydrated caesium aluminosilicate with the composition of $\text{Cs}_2\text{Al}_2\text{Si}_4\text{O}_{12}$ and rhodizite, a hydrated borate of aluminium, beryllium, sodium, and caesium ($\text{K}, \text{Cs})\text{Al}_4\text{Be}_4(\text{B}, \text{Be})_{12}\text{O}_{28}$ (Hart et al., 1975).

Rubidium is found together with caesium, and with potassium minerals such as lepidolite, which may contain the highest amount of rubidium as compared with other minerals (Faure & Powell (1972). Nevertheless, the more frequent K-bearing mineral like biotite, feldspars, and carnallites are the principal carriers of rubidium (Faure & Powell (1972).

Lithium was detected in an early industrial mineral exploration in the Tokaj mountain in a diatomite bearing lacustrine basin in volcanogenic sediments. The sporadic assays have shown a maximum Li content of 2.2 % in drill core samples (Mátyás & Várhegyi 1979). This information, along with the latest results of jadarite discoveries in Serbia - triggered an orientation survey for lithium.

2. GEOLOGICAL SETTING

Tokaj Mountain is found in the north eastern part of Hungary (Figure 1). The Bodrog and Tisza rivers, in the southeast, and the Hernád river valley, in the northwest, form its border (Balla 1980). According to (Zelenka et al., 2012), Proterozoic to Lower Palaeozoic basement outcrops can be seen in the eastern portion of Tokaj, and the Mesozoic basement has a carbonate dominance with Badenian volcanics and sediments overlain in the south.

According to (Harangi, 2001), an underwater rhyodacite-ignimbrite flow marked the start of volcanic activity in the Early Badenian. Late Badenian rhyolitic tuff outcrops can be found in the northern part, (Gyarmati, 1977). According to Gyarmati, (1977) rhyolitic pyroclasts in large masses accumulated on land, less in shallow marine environment in the Sarmatian.

There was an intense post-volcanic activity in the Late Sarmatian, which produced quartz veins and silica bodies. The latter ones formed along the paleo-groundwater table at the basement of the steam-heated alteration zone. Industrial minerals like kaolinite, bentonite, illite, diatomite, and limnic silica were produced in the hot-spring basins (Molnár & Takács, 1993). Tectonic movements split the mountains after the volcanic activity, and the outermost sections gradually sank. Along the fractures valleys and basins were formed like Erdőbénye valley basin.

The primary basin filling formation of Erdőbénye is defined as part of the Sarmatian-Lower Pannonian period. Rhyolite tuff and both fallen and reworked, as well as accumulated versions of it, make up the basin's base (Szepesi, 2013). Diatomite, limnoquartzite, clay mineral alteration (bentonite and kaolinite), accumulated rhyolitic tuff, layers of tuff and andesite make up the Erdőbénye basin formation as shown in (Figure 1, B.).

3. SAMPLING AND METHODS

In the Erdőbénye diatomite quarry field measurement, 89 samples were used for Li, Rb, and Cs analysis in which the sampling spots are shown in (Figure 1, C) in a package form. Each sample site was

measured ten times at different spot on it and taking an average of the value.

Using portable laser-induced breakdown spectroscopy, 890 measurements were taken. Following that, the concentration of the sample at each sample point was averaged.

Thirteen samples were taken from site based on their highest LIBS lithium concentration measurement and were sent to ALS Global laboratory for multi-element concentration measurement using ICP-MS analytical technique for calibration of the LIBS field results. Tables 1 and 2 show the results for ICP-MS and LIBS, respectively.

The applied ME-MS89L package is one of the ICP-MS analytical codes with the lowest detection limits, capable of measuring 2ppm-2.5% Li and other elements using digestion with Na₂O₂ fusion and ALS's super trace ICP-MS methodology. A kit suitable for exploring pegmatites in search of Li and related commodities (alsglobal.com).

4. RESULT AND DISCUSSION

Table 3 summarizes the results of the assays performed at Erdőbénye, Taylor's (1964) earth crust abundance values have been placed in the final column for comparison.

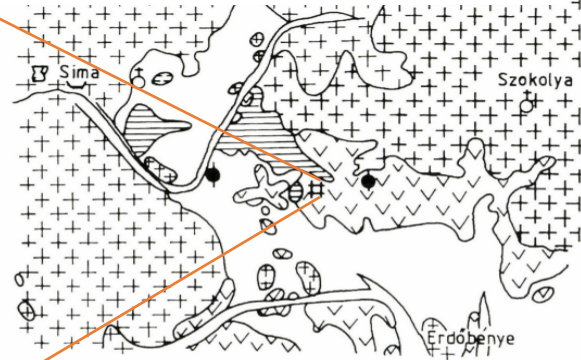
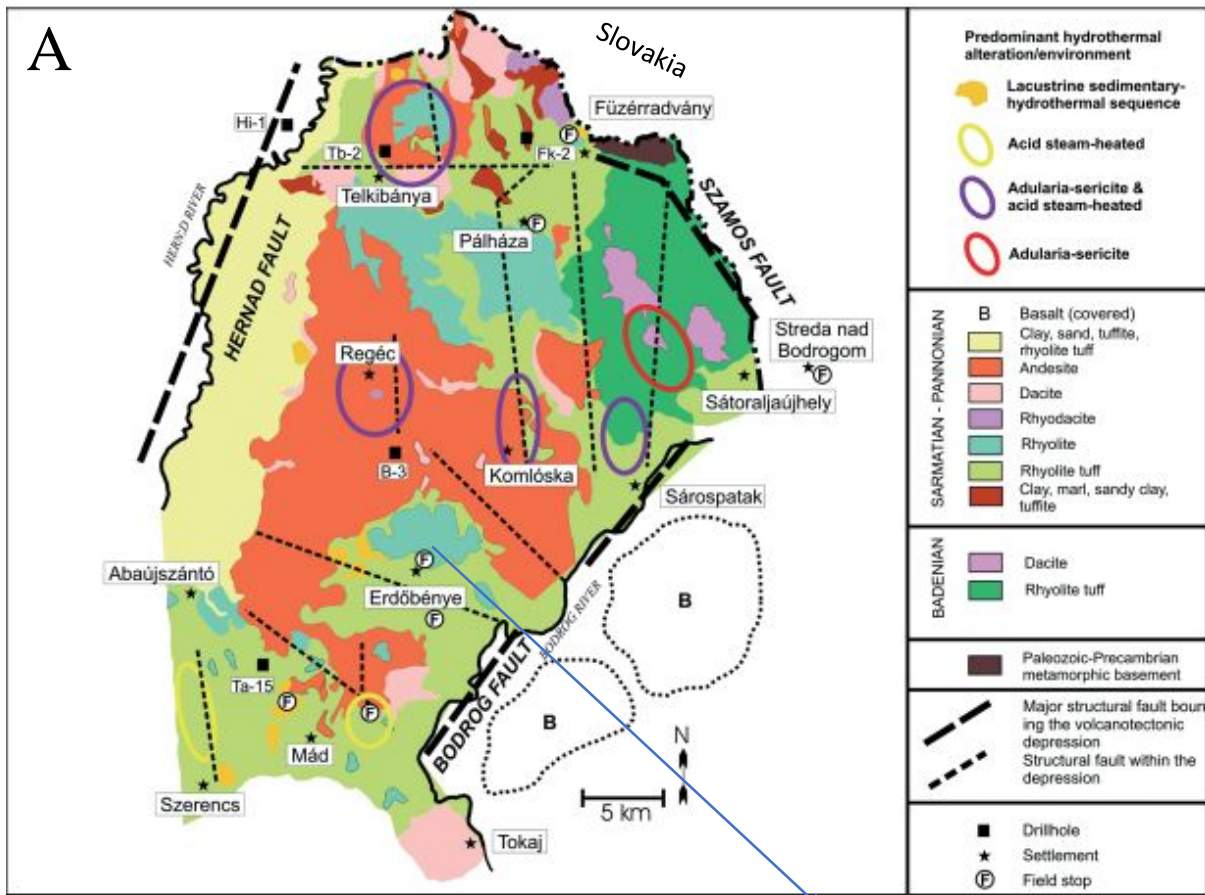
The table enables conclusions to be drawn about the accuracy of LIBS instrument field test measurements in the Erdőbénye geological environment, as well as the geochemical behaviours of alkali metals in freshwater lake environments on volcanic terrains. It should also be pointed out that the difference in sampling (laser-induced field measurements in sq.mm sized spots vs ICP-MS laboratory analysis of ground homogenized aliquot samples of several kilograms) may cause significant errors in the final acquired assay values.

4.1. Descriptive statistics of LIBS assay result

The descriptive statistical parameter for sixteen variables (K, Cs, Rb, Be, Ca, Ce, Fe, Mg, Ti, Zn, Al, Na, S, Cu, Li, and Sr) of LIBS assay results of the Erdőbénye diatomite quarry has been developed as shown in Table 4. below to clarify the base for the comparison of geochemical data. This is the set of elements provided by the calibration of the LIBS unit used in the test.

4.2. Descriptive statistics of ICP-MS assay result

The descriptive statistical parameter for twelve variables that can be detected by ICP-MS from the



C Figure 1. A. Geological map of Tokaj Mts. (Molnár et al., 2001; Molnár et al., 1995). C. Sample location

variables that are recorded by handheld spectrometry (K, Li, Cs, Rb, Be, Ca, Ce, Fe, Mg, Ti, Zn, and Sr) of ICP-MS assay results of the Erdőbénye diatomite quarry has been made, as shown in Table 5 below, to clarify the basis for the comparison of geochemical data. It was discovered that the data for Ce, Li, Cs, and Sr showed a higher variability (standard deviation). On the other hand, the other measurement has a lower variability (standard deviation), indicating that the observed values are close to the measurement's mean.

The variation in the measured Li content shows

good correlation with the variation of Ca and Mg content (Figure 2).

4.3. Correlation of the whole LIBS assay dataset

The raw data from the whole LIBS measurement was used to perform the inter-element relationship indicated by Spearman's rank correlation, as shown in Table 6, which demonstrated that the most studied elements were characterized by poor or

Table 1. ALS global ICP-MS assay results

sample ID	Be ppm	Ca %	Ce ppm	Cs ppm	Fe %	K%	Li ppm	Mg%	Rb ppm	Sr ppm	Ti %	Zn ppm	Lithology
230621-2-C	4.9	0.5	90.7	225	2.45	3.14	33	0.34	466	120	0.171	80	diatomite
240621-1-B2	3.1	1.8	48	122	1.65	0.51	41	0.6	116.5	60	0.069	60	diatomite
240621-3-B	0.9	0.1	9.7	95.4	0.27	0.18	4	0.09	35.8	30	0.024	20	diatomite
230621-1-C1	1.1	0.2	4.3	51.9	0.32	0.16	5	0.05	21.8	30	0.012	40	silica sinter
230621-1-C3	1.3	0.2	2.8	46	0.17	0.12	4	0.04	16.4	30	0.006	40	silica sinter
230621-2-B5	5.9	0.5	91.6	256	1.91	3.92	26	0.23	559	120	0.153	80	silica sinter
240621-3-A	1.7	0.3	26.2	36.2	0.62	0.15	6	0.19	16.4	40	0.018	40	silica sinter
240621-2-D2	4.9	1.1	77.6	517	1.8	2.13	32	0.68	946	120	0.096	80	tuff
230621-2-A	4.6	1.4	78.7	203	2.11	2.14	47	0.74	698	100	0.107	90	tuff
240621-2-D1	4.6	0.8	71.1	456	1.64	3.29	24	0.28	1185	90	0.081	70	tuff
230621-2-B4	3.6	0.4	58.2	237	1.14	3.62	11	0.1	520	70	0.09	50	tuffaceous sandstone
240621-1-E2	4.5	0.7	63.8	321	2.06	3.57	23	0.22	729	90	0.115	80	tuffaceous sandstone
240621-3-E	5.2	0.6	71.1	330	2.26	3.6	19	0.22	876	90	0.101	80	tuffaceous sandstone

Table 2. handheld LIBS assay results

sample ID	Be ppm	Ca %	Ce ppm	Cs ppm	Fe%	K %	Li ppm	Mg%	Rb ppm	Sr ppm	Ti %	Zn ppm	Lithology
23062021-2-C	6	0.6671	3884	264	3.792	6.8953	667	0.1282	116	297	0.2962	16	diatomite
24062021-1-B2	7	0.4502	24806	233	6.4838	6.2202	744	0.2016	68	112	0.2103	22	diatomite
24062021-3-B	7	0.4371	44460	336	4.1857	5.131	699	0.1388	140	149	0.3538	6	diatomite
23062021-1-C1	14	0.7588	1493	149	14.812	4.0846	638	0.0957	25	480	0.3499	26	silica sinter
23062021-1-C3	9	1.2536	5566	166	4.1315	3.7018	658	0.1643	15	134	0.1348	21	silica sinter
23062021-2-B5	6	0.278	270	336	4.4802	3.3088	636	0.1263	140	190	0.1148	17	silica sinter
24062021-3-A	5	0.745	785	200	5.7663	2.7368	649	0.1127	12	109	0.1021	27	silica sinter
24062021-2-D2	5	0.8506	7539	277	4.7505	4.216	654	0.176	111	254	0.1759	7	tuff
23062021-2-A	7	0.3271	23654	292	3.8371	6.2422	667	0.1729	85	140	0.3129	11	tuff
24062021-2-D1	7	0.92500	7202	200	4.853	4.9036	645	0.1089	28	134	0.1206	12	tuff
23062021-2-B4	7	0.1793	5168	301	4.7793	5.2473	635	0.109	121	272	0.1976	23	tuffaceous sandstone
24062021-1-E2	6	0.8818	2096	184	6.6577	3.0204	636	0.1125	58	113	0.1155	23	tuffaceous sandstone
24062021-3-E	9	0.3911	27040	275	3.9195	9.2502	697	0.1706	86	125	0.6127	9	tuffaceous sandstone

significantly lower correlation coefficients. The remaining components, which are depicted in green, have high correlation coefficients.

Table 3. relations between Average assay results of ICP-MS and LIBS

	ICP-MS	LIBS (ICP-MS equivalent)	Whole LIBS result	Av. crustal abundance*
No. of samples	13	13	890	-
Be ppm	3.6	7.3	14.0	3.0
Ca %	0.7	0.6	1.1	4.2
Ce ppm	53.4	11843.3	11164.0	46.0
Cs ppm	222.8	247.2	312.0	3.0
Fe %	1.4	5.6	4.2	5.6
K %	2.0	5.0	4.2	2.1
Li ppm	21.2	663.5	483.0	20.0
Mg %	0.3	0.1	0.2	2.3
Rb ppm	475.8	77.3	61.0	90.0
Sr ppm	76.2	193.0	168.0	375.0
Ti %	0.1	0.2	0.3	0.6
Zn ppm	62.3	16.9	15.0	70.0
Cu ppm	10	15.5	32.0	55.0
S %	nd	1.3	2.0	43.0
Na %	nd	0.2	0.2	2.4
Al %	nd	10.6	7.7	8.2

*Source (Taylor, 1964), Av. Average. nd: not evaluated during measurement.

In this table, both Be and Cu are showing a positive correlation with Cs. Contrarily, there is a poor correlation between Ca and Cs. There is a positive correlation between Rb and Al. Li content has no any correlation with the investigated components. According to Suresh et al., (2011), if the correlation coefficient between the metals is larger, the metals have similar behaviour during transport, having common sources, and mutual dependency. The lack of correlation indicates that the contents of these elements are controlled by a combination of geochemical support phases and their mixed associations.

4.4. The accuracy of the LIBS method

According the parallel results, the four measured comparable alkali elements (K, Li, Rb, Cs) gave different responses. The best fit was observed in the case of Cs cesium, with less than 10 % variation between the ICP-MS and LIBS averages. Moderate deviation was detected in the case of potassium (2.5-times higher averages in LIBS than ICP-MS). Large deviation was found in the case of Li and Rb (Li lithium is 30 times overestimated compared to ICP-MS values, while Rb rubidium is 7 times underestimated

by the LIBS compared to the ICP-MS values).

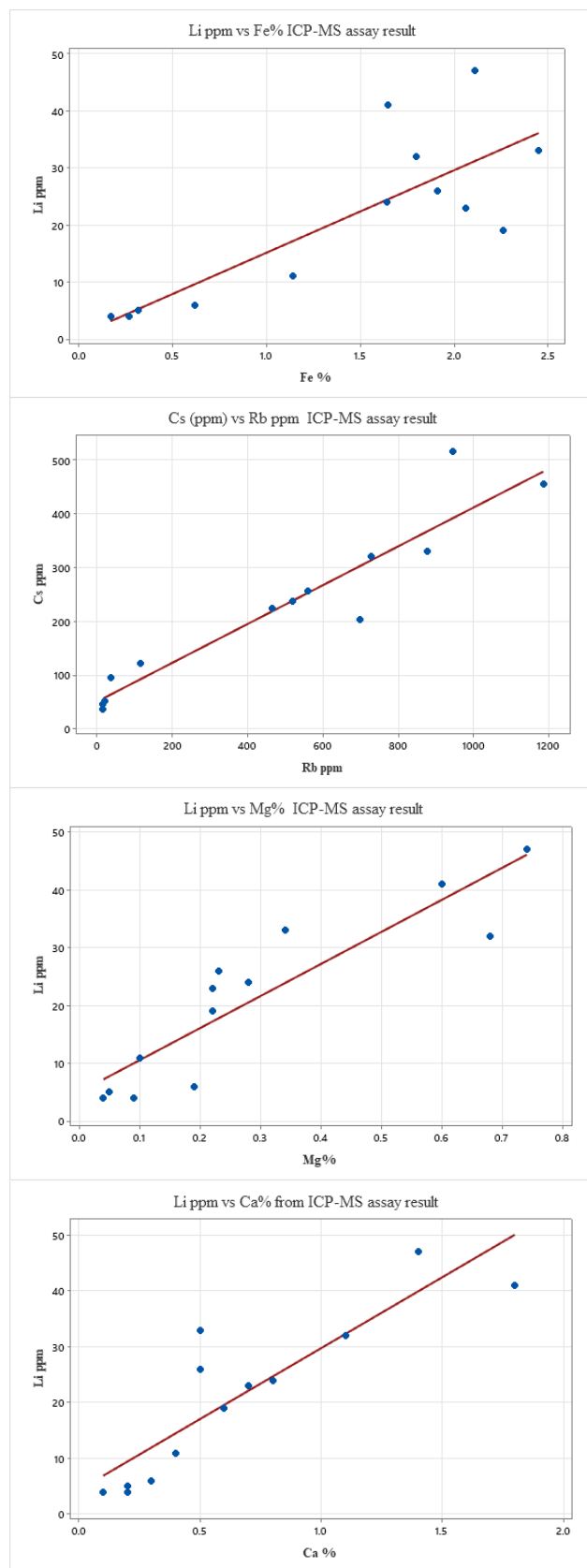


Figure 2. Graphs of some highly inter-related elements from ICP-MS assay result.

Table 4. Descriptive statistics of the whole LIBS measurements

Variable	Total Count	Mean	St. Dev	Minimum	Median	Maximum	Skewness	Kurtosis
Li ppm	890	479.60	145.10	168.00	482.00	1049.00	0.52	1.33
K %	890	43.78	18.98	7.95	41.26	108.10	0.64	0.52
Cs ppm	890	323.10	105.30	108.00	320.00	531.00	0.03	-0.74
Rb ppm	890	59.61	48.61	9.00	44.00	279.00	2.00	5.54
Al %	890	70.52	39.56	14.65	72.30	168.83	0.30	-0.78
Be ppm	890	15.05	7.49	5.00	13.00	35.00	0.51	-0.74
Ca %	890	9.21	18.41	0.14	2.92	115.69	3.67	15.53
Ce %	890	12.07	16.83	0.08	6.20	83.90	2.54	6.94
Cu ppm	890	33.46	15.20	11.00	31.00	74.00	0.47	-0.76
Fe %	890	39.06	16.92	14.95	35.10	148.12	3.44	19.02
Mg %	890	1.92	0.94	0.67	1.76	7.80	3.17	17.14
Na %	890	1.42	1.05	0.46	1.24	9.71	5.82	43.85
S %	890	19.84	8.45	5.69	18.25	41.28	0.56	-0.48
Sr ppm	890	160.10	129.00	70.00	121.00	1076.00	4.64	28.99
Ti %	890	2.99	1.99	0.49	2.56	9.02	1.09	0.62
Zn ppm	890	15.06	8.59	4.00	12.00	48.00	1.51	2.95

Table 5. Descriptive statistics of ICP-MS result

Variable	Mean	St. Dev	Min.	Median	Max.	Skewness	Kurtosis
Li ppm	21.15	14.55	4.00	23.00	47.00	0.30	-1.04
K, %	2.04	1.59	0.12	2.14	3.92	-0.23	-1.96
Cs ppm	222.80	154.20	36.20	225.00	517.00	0.54	-0.50
Rb ppm	476.00	404.00	16.00	520.00	1185.00	0.20	-1.23
Be ppm	3.56	1.75	0.90	4.50	5.90	-0.49	-1.40
Ca, %	0.66	0.50	0.10	0.50	1.80	1.17	0.83
Ce ppm	53.37	32.25	2.80	63.80	91.60	-0.59	-1.18
Fe, %	1.42	0.81	0.17	1.65	2.45	-0.50	-1.38
Mg, %	0.29	0.24	0.04	0.22	0.74	0.98	-0.28
Sr ppm	76.15	35.25	30.00	90.00	120.00	-0.16	-1.52

Table 6. Spearman's correlation matrix of the whole LIBS assay results. The unit is ppm for all of the elements

Elements	Li	K	Cs	Rb	Al	Be	Ca	Ce	Cu	Fe	Mg	Na	S	Sr	Ti
K	0.252														
Cs	-0.286	0.128													
Rb	0.221	0.003	-0.089												
Al	0.297	-0.364	-0.455	0.629											
Be	-0.329	0.166	0.851	-0.343	-0.682										
Ca	-0.155	-0.435	-0.512	-0.141	-0.027	-0.382									
Ce	0.153	0.572	0.156	-0.066	-0.441	0.224	-0.150								
Cu	-0.393	-0.005	0.787	-0.401	-0.673	0.956	-0.225	0.144							
Fe	0.315	-0.160	-0.430	0.129	0.503	-0.404	-0.054	-0.226	-0.373						
Mg	-0.196	-0.045	-0.185	-0.117	-0.005	-0.143	0.059	-0.006	-0.136	-0.066					
Na	0.113	0.090	-0.091	-0.095	-0.039	-0.026	-0.058	0.053	-0.070	0.089	-0.008				
S	-0.240	-0.031	0.498	-0.052	-0.247	0.519	-0.158	0.037	0.511	-0.304	-0.202	-0.002			
Sr	0.089	-0.220	-0.424	-0.078	-0.041	-0.293	0.689	-0.091	-0.180	0.085	-0.059	-0.084	-0.144		
Ti	0.002	0.698	0.498	-0.140	-0.598	0.595	-0.393	0.611	0.495	-0.278	-0.106	0.013	0.222	-0.285	
Zn	0.121	-0.066	-0.025	0.157	0.273	0.031	-0.211	-0.223	0.079	0.304	-0.144	0.081	-0.012	-0.181	-0.016

Remark: positive correlation coefficient greater than 0.5 are coloured by grey
 Negatively correlation coefficient less than -0.5 are coloured by red

411

Table 7. concentration of elements from the LIBS reading with Lithological distribution

Lithology	Amount of sample	Li ppm	Cs ppm	Rb ppm	K %	Al %	Ca %	Fe %	Mg %	Na %	S %	Ti %	Be ppm	Ce %	Cu ppm	Sr ppm	Zn ppm
Clay	25	488	306	61	4.05	7.58	0.77	3.99	0.23	0.15	1.81	0.25	14	0.70	32	141	17
Tuff and Tuffite	14	501	349	82	4.98	7.61	0.55	3.99	0.17	0.13	2.09	0.31	16	0.93	33	157	14
Tuffaceous sandstone	13	524	302	78	4.52	8.94	0.63	4.41	0.17	0.11	2.04	0.28	13	1.18	28	143	17
Silica sinter	8	457	248	39	2.65	9.26	2.92	5.22	0.16	0.25	1.76	0.18	11	0.30	26	232	16
Diatomite	29	447	355	45	4.79	4.87	0.81	3.21	0.19	0.13	2.12	0.38	17	2.04	39	166	13

Further substantial discrepancies were seen in the case of Ce cerium, with LIBS values being more than two magnitudes higher than ICP-MS readings. This deviation may lead the drawing of false conclusion to have REE anomaly, which does not exist in reality. This emphasizes the importance of further careful adjustment of equipment preliminary calibration to match the unique regional geological environment.

4.5. Relation of the two-assay result and average crustal concentration

Table 1 allows drawing conclusions both the accuracy of the field test measurements of LIBS instrument in the Erdobénye geological environment, and for the geochemical behaviour of alkali metals in the freshwater lake environment on volcanic terrains.

4.5.1. The average values compared to crustal abundances

The tests brought different results. Cs cesium enrichment is 74-82 times that of the crustal average. Li and Rb enrichment is ambiguous, i.e. Li is anomalous in the LIBS dataset (33 times crustal average), while it is not in the ICP-MS. Rubidium is anomalous in the ICP-MS dataset (more than 5 times crustal average) while it stays around the crustal average in the case of LIBS assays.

4.5.2. Lithological enrichment of elements based on LIBS

The searched elements (Li, Cs, Rb, and K) are most abundant in clay, tuff and tuffite, and tuffaceous sandstone lithological units. The concentration of Li is highest in tuffaceous sandstone, tuff and tuffite and clay in descending order. The caesium Cs in descending order: tuff and tuffite, clay and tuffaceous sandstone. Furthermore, tuff and tuffite, tuffaceous sandstone and clay contain the highest concentration of Rb in the basin. All the detected elements which are measured by handheld LIBS spectrometry with respect to classified lithological profiles of Erdőbénye basin is shown in the Table 7.

5. CONCLUSION

The Erdőbénye diatomite area is a sedimentary basin composed of volcanoclastic and lacustrine sediments. Early indicated a potential enrichment of lithium and triggered and orientational survey.

In this survey two analytical methods (LIBS on-site measurement and ICP-MS assay) were used to determine the element concentrations in this area.

Based on the results of the two assays, the

possible use of LIBS spectrometer was evaluated in detail for the field determination of K, Li, Rb, Cs elements.

There are significant differences between the assay results, as is made clear in the result and discussion above. Without through previous calibration the field LIBS may produce false readings, erroneously evaluated as geochemical anomalies. The calibration needs skilled expertise.

During our published measurement, it was calibrated using the laboratory provided standard. Between the LIBS result and the ICP-MS result, this calibration issue caused a significant discrepancy.

It is recommended to run a preliminary test measurement and sampling series using assayed samples from the same site to improve the applicability of this very promising exploration tool.

REFERENCES

- Balla Z.**, 1980. *Neogene volcanites in the geodynamic reconstruction of the Carpathian region.* – Geophysical Transactions, Vol. 26
- Erdei B.**, 1995, *The Sarmatian flora from Erdőbénye-Ligetmajor, NE Hungary*, *Annls. hist.-nat. Mus. natu. hung.* 87: 11-33
- Faure G., & Powell J.L.**, 1972. *The Geochemistry of Rubidium and Strontium. In: Strontium Isotope Geology. Minerals, Rocks and Inorganic Materials*, vol 5. Springer, Berlin, Heidelberg. https://doi.org/10.1007/978-3-642-65367-4_1
- Grant, A.**, 2019, *The Sedimentary Lithium Opportunity 7.* The Sedimentary Lithium Opportunity — Jade Cove Partners
- Gyarmati P.**, 1977. *Intermediate volcanism in the Tokaj Mts.* *MÁFI Évkönyve*, 58: 1–196
- Harangi S.**, 2001. *Neogene magmatism in the Alpine-Pannonian Transition Zone—a model for melt generation in a complex geodynamic setting* *Acta Vulcanologica*, 13/1, 25-39
- Hart W.A., Beumel, O.F., & Whaley, T.P.**, 1973. *The chemistry of lithium, Sodium, potassium, rubidium, cesium and francium.* Pergamon texts in inorganic chemistry <https://doi.org/10.1016/C2013-0-05695-2> <https://www.alsglobal.com/en/geochemistry/energy-minerals-analysis/lithium> Lithium (alsglobal.com), Accessed 11-May-23
- Mátyás E. & Várhegyi G.** 1979, *yelenetés a Tokaji-hegység inthofeim intatan hedméyeiol (in Hungarian).*
- Molnár F. & Takács J.**, 1993. *Silica4 minerals of Mulató Hill, Erdőbénye (NE Hungary).* *Topographia Mineralogica Hungariae*, 1: 19–40
- Molnár, F., Nagymarosy, A., Jeleň, S., & Bačo, P.**, (2010), *Minerals and wines: Tokaj Mts., Hungary and Slanské vrchy Mts., Slovakia. In: Acta mineralogica-petrographica, (15). pp. 1-40.* <http://acta.bibl.u-szeged.hu/46898/>
- Senesi G.S.**, 2017. *Portable Handheld Laser-induced Breakdown Spectroscopy (LIBS) Instrumentation*

for in-field Elemental Analysis of Geological Samples. *Int J Earth Environ Sci* 2: 146. doi: <https://doi.org/10.15344/2456-351X/2017/146>

Suresh G, Ramasamy V, Meenakshisundaram V, Venkatachalapathy R, & Ponnusamy V., 2011. Influence of mineralogical and heavy metal composition on natural radionuclide contents in the river sediments. *Appl. Radiat. Isot.* 69, 1466–1474. <https://doi.org/10.1016/j.apradiso.2011.05.020>

Szepesi J., 2013. A Tokaji-hegység és Telkibánya környezetének földtani viszonyai (in Hungarian).

Talens Peiró, L., Villalba Méndez, G., & Ayres, R.U.,

2013. *Lithium: Sources, Production, Uses, and Recovery Outlook.* *JOM* 65, 986–996. <https://doi.org/10.1007/s11837-013-0666-4>

Taylor S.R., 1964. Abundance of chemical elements in the continental crust: a new table. *Geochimica et Cosmochimica Acta* 28, 1273–1285. [https://doi.org/10.1016/0016-7037\(64\)90129-2](https://doi.org/10.1016/0016-7037(64)90129-2)

Zelenka, T., Gyarmati, P., & Kiss, J., 2012. Paleovolcanic reconstruction in the Tokaj Mountains. *Central European Geology* 55, 49–83. <https://doi.org/10.1556/CEuGeol.55.2012.1.4>

Received at: 24. 05. 2023

Revised at: 07. 08. 2023

Accepted for publication at: 12. 08. 2023

Published online at: 16. 08. 2023